EUROPEAN ORGANIZATION FOR NUCLEAR RESEARCH

CERN-PPE/92–121
21 July 1992

Measurement of the $e^+e^-\rightarrow b\bar{b}$ and $e^+e^-\rightarrow c\bar{c}$ Forward-Backward Asymmetries at the Z^0 Resonance

The L3 Collaboration

Abstract

We have measured the forward-backward asymmetry in $e^+e^- \rightarrow b\bar{b}$ and $e^+e^- \rightarrow c\bar{c}$ processes using hadronic events containing muons or electrons. The data sample corresponds to 410,000 hadronic decays of the Z^0. From a fit to the single lepton and dilepton p and p_T spectra, we determine

$$A_{b\bar{b}} = 0.086 \pm 0.015 \pm 0.007$$
and
$$A_{c\bar{c}} = 0.083 \pm 0.038 \pm 0.027$$

at the effective center-of-mass energy $\sqrt{s} = 91.24$ GeV. These measurements yield a value of the electroweak mixing angle

$$\sin^2\overline{\theta}_W = 0.2336 \pm 0.0029.$$

(Submitted to Physics Letters B)

Introduction

The forward-backward asymmetry of quark pairs, $A_{\mathrm{q\bar{q}}}$, produced in the $\mathrm{e^+e^-} \to \mathrm{Z^0} \to \mathrm{q\bar{q}}$ process is sensitive to the electroweak mixing angle, $\sin^2\theta_{\mathrm{W}}$, which is one of the fundamental parameters of the Standard Model [1]. The forward-backward asymmetry for the process $\mathrm{e^+e^-} \to \mathrm{q\bar{q}}$ is defined as

$$A_{\mathrm{q\bar{q}}} = \frac{\sigma_F^q - \sigma_B^q}{\sigma_F^q + \sigma_B^q} \tag{1}$$

where σ_F^q and σ_B^q are the cross-sections in the forward and backward hemispheres with respect to the electron beam. In the Standard Model using the improved Born approximation framework [2,3] the asymmetry on the $\mathrm{Z^0}$ peak is given by

$$A_{\mathrm{q\bar{q}}}^{\mathrm{Born}} \equiv \frac{3}{4} A_{\mathrm{e}} A_{\mathrm{q}}, \tag{2}$$

where

$$A_i = \frac{2 v_i a_i}{v_i^2 + a_i^2} = \frac{2(1 - 4 \mid Q_i \mid \sin^2\overline{\theta}_{\mathrm{W}})}{1 + (1 - 4 \mid Q_i \mid \sin^2\overline{\theta}_{\mathrm{W}})^2}. \tag{3}$$

Here v_i, a_i and Q_i are the vector and axial-vector coupling constants and the charge of the electron or quark, and $\sin^2\overline{\theta}_{\mathrm{W}}$ is the effective electroweak mixing angle at the $\mathrm{Z^0}$ mass. The resulting angular distribution of the quark is

$$\frac{d\sigma}{d\cos\theta} \propto \frac{3}{8}(1 + \cos^2\theta) + A_{\mathrm{q\bar{q}}} \cos\theta, \tag{4}$$

where θ is the polar angle of the quark with respect to the electron beam.

In this letter we present measurements of $A_{\mathrm{b\bar{b}}}$ and $A_{\mathrm{c\bar{c}}}$. We use electrons and muons from the semileptonic decay of b- or c-quarks to select events coming from $\mathrm{Z^0} \to \mathrm{b\bar{b}}$ and $\mathrm{Z^0} \to \mathrm{c\bar{c}}$. Because of the hard fragmentation and large mass of the b-quark, leptons from b-quark decay have large momentum, p, and large transverse momentum, $p_{_T}$, with respect to the quark direction. The c-quark, with its lower mass and softer fragmentation, produces leptons with lower p and $p_{_T}$, but nevertheless still higher than that of leptons from the decays of the lighter quarks. As the charge of the lepton is correlated with the charge of the quark, we can use events containing these inclusive leptons to measure $A_{\mathrm{b\bar{b}}}$ and $A_{\mathrm{c\bar{c}}}$. We use the thrust axis of the event to give the direction of the quark and we tag its charge with the lepton charge. To determine $A_{\mathrm{b\bar{b}}}$ and $A_{\mathrm{c\bar{c}}}$, we perform a maximum likelihood fit to the single lepton and dilepton p and $p_{_T}$ spectra. Similar analyses have previously been performed with lower statistics [4–8].

Due to mixing in the $\mathrm{B^0}$-$\mathrm{\bar{B}^0}$ system, the observed b-quark asymmetry, $A_{\mathrm{b\bar{b}}}^{\mathrm{obs}}$, is smaller than the actual asymmetry by a factor $(1-2\chi_{_\mathrm{B}})$, where $\chi_{_\mathrm{B}}$ is the probability that a hadron containing a b-quark had oscillated into a hadron containing a $\bar{\mathrm{b}}$-quark at the time of its decay. We have reported a measurement of $\chi_{_\mathrm{B}}$ in a previous letter [9]. As there is no observable mixing with D mesons, $A_{\mathrm{c\bar{c}}}$ is measured directly.

Our data sample consists of 410,000 hadronic events corresponding to 17.6 $\mathrm{pb^{-1}}$ collected in 1990 and 1991 on or near the $\mathrm{Z^0}$ resonance using the L3 detector at LEP. The center-of-mass energies are distributed over the range $88.2 \leq \sqrt{s} \leq 94.2$ GeV.

The L3 Detector

The L3 detector covers 99% of 4π. The detector consists of a central tracking chamber, a high resolution electromagnetic calorimeter composed of BGO crystals, a ring of scintillation counters, a uranium and brass hadron calorimeter with proportional wire chamber readout, and an accurate muon chamber system. These detectors are installed in a 12 m diameter magnet which provides a uniform field of 0.5 T along the beam direction.

The central tracking chamber is a time expansion chamber which consists of two cylindrical layers of 12 and 24 sectors, with 62 wires measuring the R-ϕ coordinate. The single wire resolution is 58 μm averaged over the entire cell. The double-track resolution is 640 μm. The fine segmentation of the BGO detector and the hadron calorimeter allows us to measure the direction of jets with an angular resolution of 2.5°, and to measure the total energy of hadronic events from Z^0 decay with a resolution of 10%. The muon detector consists of 3 layers of precise drift chambers which measure 56 points on the muon trajectory in the bending plane, and 8 points in the non-bending direction.

For the present analysis, we use the data collected in the following ranges of polar angles:

- for the central chamber, $41° < \theta < 139°$,
- for the hadron calorimeter, $5° < \theta < 175°$,
- for the muon chambers, $35.8° < \theta < 144.2°$,
- for the electromagnetic calorimeter, $11° < \theta < 169°$.

A detailed description of each detector subsystem, and its performance, is given in Reference 10.

Selection of Inclusive Lepton Events

The trigger requirements and the selection criteria for hadronic events containing electrons and muons have been described earlier [9, 11]. Muons are identified and measured in the muon chamber system. We require that a muon track consist of track segments in at least two of the three layers of muon chambers, and that the muon track point to the intersection region. Electrons are identified using the BGO and hadron calorimeters, as well as the central tracking chamber. We require an energy cluster in the BGO that is consistent with the shape of an electromagnetic shower and which matches in ϕ angle and momentum with a track in the central tracking chamber. For this analysis, we have only considered electrons in the barrel region ($|\cos\theta| < 0.69$). We reject hadrons misidentified as electrons by requiring that there be less than 3 GeV deposited in the hadron calorimeter in a cone of half angle 7° behind the electromagnetic cluster. The charge of the electron is determined from the tracking chamber. The shower shape and hadron calorimeter criteria select electrons that are isolated from nearby particles, resulting in a lower efficiency for electrons than for muons.

The momentum of muon candidates is required to be at least 4 GeV, while the electrons are required to have at least 3 GeV. Table 1 shows the number of single lepton and dilepton events obtained after all cuts.

To determine the acceptance for inclusive lepton events, we use the JETSET parton shower program [12] with string fragmentation. For b- and c-quarks we use the Peterson fragmentation function [13] as a function of $x_E = 2E_{\mathrm{hadron}}/\sqrt{s}$ with the parameters $\epsilon_{\mathrm{b}} = 0.05$ and $\epsilon_{\mathrm{c}} = 0.50$. The generated events are passed through the L3 detector simulation [14], which includes the effects of energy loss, multiple scattering, interactions and decays in the detector materials and beam pipe. We use the average of the semileptonic branching ratios measured by previous

Type	Events
μ + hadrons	20937
e + hadrons	5443
$\mu\mu$ + hadrons	1083
ee + hadrons	152
μe + hadrons	709

Table 1: Number of inclusive lepton events

experiments [15,16]:[1)] $\mathrm{Br}(b \to \ell) = 0.117 \pm 0.006$ and $\mathrm{Br}(c \to \ell) = 0.096 \pm 0.006$. We assume that the mixture of c-hadrons from the cascade decay $b \to c$ is the same as that in $Z^0 \to c\bar{c}$, and so we use the measured $c \to \ell$ branching ratio also for $b \to c \to \ell$, after taking into account the additional c-quarks coming from W decays. We determine that the efficiency for observing a prompt $b \to \ell$ decay is 42.5% for muons and 23.3% for electrons.

Monte Carlo events with leptons are classified into six categories: $b \to \ell$, $b \to c \to \ell$, $b \to \tau \to \ell$, $b \to c\bar{c}s$ where $\bar{c} \to \ell$, $c \to \ell$, and background. Included in the background are leptons from π and K decays, Dalitz decays, photon conversions, and misidentified hadrons caused by, for example, $\pi - \gamma$ overlap for electrons and punchthrough for muons. Table 2 shows the results of Monte Carlo studies giving the fraction of each source of leptons and background for data samples with no cut on transverse momentum and also with a cut at 1.0 GeV. The transverse momentum is defined with respect to the nearest jet [17], where the measured energy of the lepton is excluded from the jet. If there is no jet with an energy greater than 6 GeV remaining in the same hemisphere as the lepton, then the p_T is calculated relative to the thrust axis of the event.

Category	μ		e	
	$p_T > 0$ GeV	$p_T > 1$ GeV	$p_T > 0$ GeV	$p_T > 1$ GeV
1: $b \to \ell$	36.5%	70.5%	67.6%	79.8%
2: $b \to c \to \ell$	10.8%	6.6%	6.6%	4.3%
3: $b \to \tau \to \ell$	1.8%	1.8%	2.5%	2.0%
4: $b \to \bar{c} \to \ell$	1.3%	0.6%	0.7%	0.4%
5: $c \to \ell$	16.1%	6.3%	4.3%	2.5%
6: background	33.5%	14.0%	18.3%	11.1%

Table 2: Monte Carlo estimates of the fraction of each process in the data sample. Also shown is the expected asymmetry for each process.

As can be seen from Table 2, the data at high p_T for both electrons and muons are dominated by events containing b-quarks. At low p_T the muon sample has a relatively large contribution from c-quarks. This is also illustrated in Figure 1 which shows the angular distribution of the thrust axis for low and high p_T events. The requirements of the electron selection result in a reduced efficiency for low p_T events, and hence for c-quark events.

[1]The notation $b \to \ell$ means the decay of a hadron containing a b-quark into a lepton (plus its neutrino) and anything else. Similarly for $c \to \ell$, *etc.* Charge-conjugate processes are also implied.

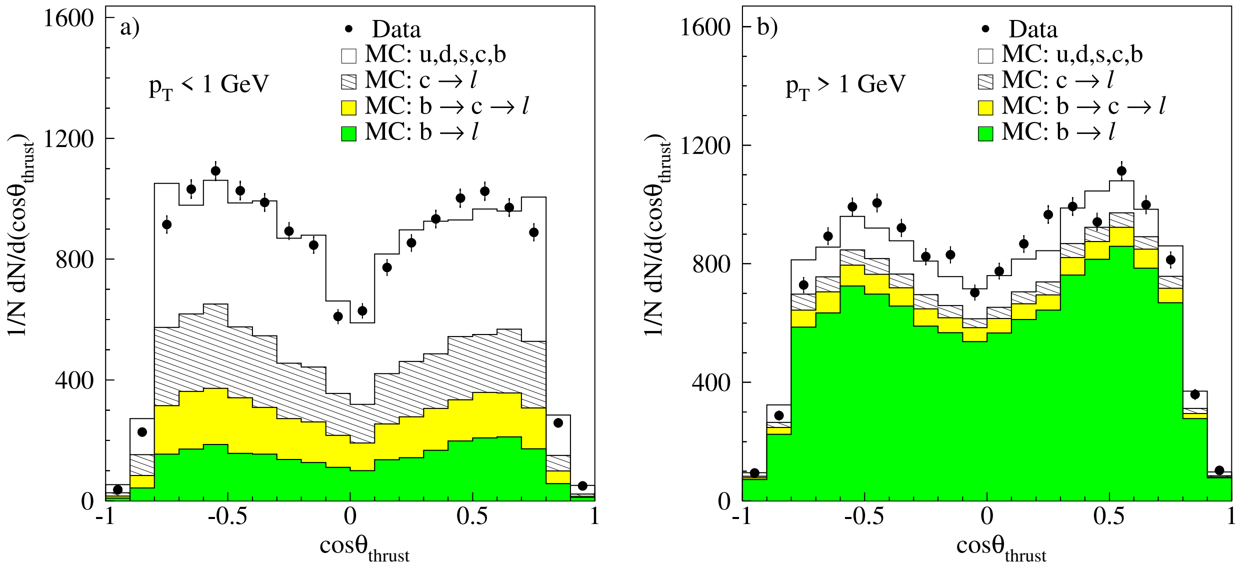

Figure 1: The measured angular distribution of the thrust axis for events containing a low p_T (< 1 GeV) lepton (a) or a high p_T lepton (> 1 GeV) (b). The contributions of the various sources are indicated.

Determination of the Forward-Backward Asymmetries

In the semileptonic decay of a b- or c-quark the charge of the detected lepton is directly correlated with the charge of the quark. We use the thrust axis to estimate the direction of the original quark. The thrust axis is oriented towards the hemisphere containing the negatively charged lepton (or opposite the positively charged lepton). With this convention, the thrust axis points in the direction of the b-quark for $\mathrm{b\bar{b}}$ events and in the direction of the $\bar{\mathrm{c}}$-quark for $\mathrm{c\bar{c}}$ events.

We first investigate the angular distribution of the thrust axis for high p_T (> 1 GeV) events. In this way, we can make a direct measurement of $A_{\mathrm{b\bar{b}}}^{\mathrm{obs}}$. The data are corrected for angular acceptance, and the non-b-quark background is subtracted. The resulting distribution is shown in Figure 2. A fit is made to the form:

$$\frac{3}{8}(1 + \cos^2\theta_{\mathrm{thrust}}) + A_{\mathrm{b\bar{b}}}^{\mathrm{obs}} \cos\theta_{\mathrm{thrust}}. \qquad (5)$$

The result is $A_{\mathrm{b\bar{b}}}^{\mathrm{obs}} = 0.062 \pm 0.013$ with $\chi^2/\mathrm{dof} = 26/19$. This method, however, has the disadvantage that the p and p_T of the lepton are not used, thus reducing sensitivity. In addition, this method is best suited to situations where the background is small, and is therefore unsuitable for a measurement of $A_{\mathrm{c\bar{c}}}$.

To use the full statistics and improve the sensitivity, we determine $A_{\mathrm{b\bar{b}}}$ and $A_{\mathrm{c\bar{c}}}$ using a non-binned maximum likelihood fit in the p versus p_T plane. The fitting procedure has been described in detail previously [5]. The probability for a data event to come from the various sources listed in Table 2 is determined from the number and type of Monte Carlo events found in a rectangular box centered on the (p, p_T) values of the data event. The weights for the likelihood function are determined by the expected angular distribution given the polar angle of the thrust axis of the data event, and the asymmetry of the possible sources of the event. For sources 1, 3 and 4, the asymmetry is $A_{\mathrm{b\bar{b}}}$, while for source 2 it is $-A_{\mathrm{b\bar{b}}}$, as the lepton from

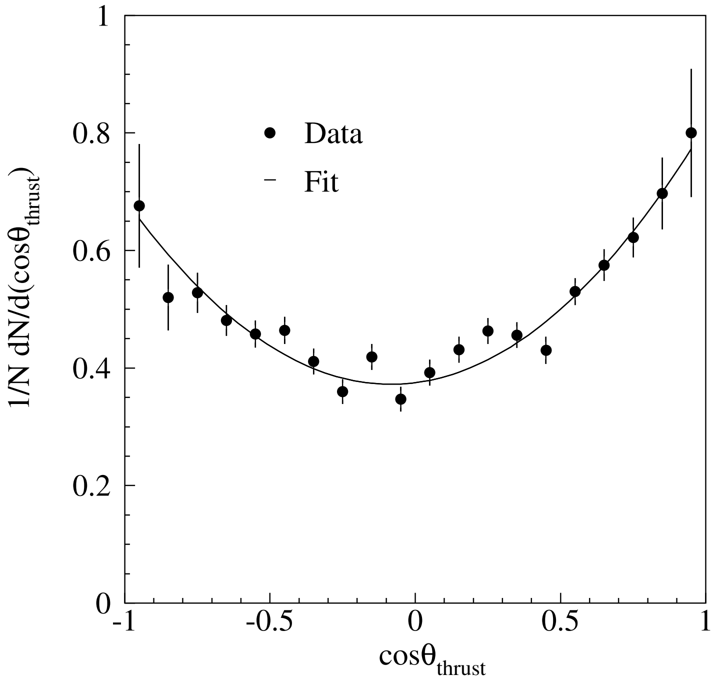

Figure 2: The angular distribution of the thrust axis for events containing high p_T leptons. The orientation of the thrust axis has been described in the text. The points are the data, and the solid line is the result of the fit.

the cascade has the opposite sign than the b-quark. For source 5, it is $-A_{c\bar{c}}$, as the thrust axis points in the direction of the $\bar{c}$-quark. In the case of dilepton events, the average asymmetries of the two leptons are used.

From a sample of $Z^0 \to \tau^+\tau^-$ events we estimate the charge confusion to be $0.2 \pm 0.2\%$ for muons and $0.8 \pm 0.3\%$ for electrons. We correct for the effects of the charge confusion, and account for its error in the systematic error.

The result of the fit for $A_{b\bar{b}}$ and $A_{c\bar{c}}$ using both inclusive muons and electrons and all center-of-mass energies is $A^{obs}_{b\bar{b}} = 0.066 \pm 0.011$ and $A_{c\bar{c}} = 0.083 \pm 0.038$. As the acceptance for $c \to e$ events is small, the $A_{c\bar{c}}$ measurement is determined almost completely by the inclusive muon events. The correlation coefficient between $A^{obs}_{b\bar{b}}$ and $A_{c\bar{c}}$ is 20%. Separate fits for $A_{b\bar{b}}$ using the muon and electron data yield $A^{obs}_{b\bar{b}} = 0.074 \pm 0.014$ for muons, and 0.053 ± 0.019 for electrons.

Table 3 lists the contributions to the systematic error in the $A^{obs}_{b\bar{b}}$ and $A_{c\bar{c}}$ measurements. We have estimated the error by changing the parameters by their known (or estimated) uncertainties. The $c \to \ell$ branching ratio error has been increased to ± 0.012 to allow for uncertainties in the $b \to c\bar{c}s$ branching ratio, as well as a possible different mixture of $D^{\pm}$ and D^0 mesons in b-quark decays. The charge of the background can be correlated with the charge of the original quark, and therefore background processes could affect the measured asymmetry. We estimate this correlation to be 0.35 ± 0.15 for background from b-quarks, and negligible for the lighter quarks. The background asymmetry for non-b-quark sources was determined from Monte Carlo studies to be consistent with zero. The error on this estimate is 0.015 which gives the dominant systematic error for $A_{c\bar{c}}$. We have estimated the effect of reconstruction errors by smearing the momentum of each lepton by 5%. The effects of jet angular resolution have been studied by smearing the jet directions in the Monte Carlo with a Gaussian distribution with a width between 0° and 1°.

Contribution	Variation	$\Delta A^{obs}_{b\bar{b}}$	$\Delta A_{c\bar{c}}$
b $\rightarrow \ell$ branching ratio	± 0.006	0.0006	0.002
c $\rightarrow \ell$ branching ratio	± 0.012	0.0013	0.013
$\Gamma_{b\bar{b}}$	± 10 MeV	0.0003	0.001
$\Gamma_{c\bar{c}}$	± 10 MeV	0.0002	0.002
background fraction	± 0.15	0.0006	0.003
background asymmetry	± 0.015	0.0006	0.020
charge correlation for b-quark background	± 0.15	0.0004	0.001
b-quark fragmentation parameter ϵ_b	± 0.006	0.0002	0.002
c-quark fragmentation parameter ϵ_c	± 0.200	0.0006	0.004
smearing the lepton momentum $\Delta p/p$	5%	0.0001	0.001
smearing the angle between the lepton and nearest jet	$0° - 1°$	0.0010	0.004
uncertainty in the charge confusion correction	± 0.0015	0.0002	0.001
Monte Carlo statistics		0.0035	0.009
Total		0.004	0.027

Table 3: Systematic errors in the $A^{obs}_{b\bar{b}}$ and $A_{c\bar{c}}$ measurements.

Our result for $A_{c\bar{c}}$ is

$$A_{c\bar{c}} = 0.083 \pm 0.038(\text{stat}) \pm 0.027(\text{sys}).$$

Due to mixing in the B^0-$\bar{B}^0$ system, the observed $b\bar{b}$ asymmetry is $A^{obs}_{b\bar{b}} = A_{b\bar{b}}(1 - 2\chi_B)$. Correcting $A^{obs}_{b\bar{b}}$ using our measured value $\chi_B = 0.121 \pm 0.017(\text{stat}) \pm 0.006(\text{sys})$ [9] we obtain

$$A_{b\bar{b}} = 0.086 \pm 0.015(\text{stat}) \pm 0.007(\text{sys}).$$

As the asymmetry is predicted to depend on the center-of-mass energy, we also have divided our data into energies below, on, and above the Z^0 resonance. The results for $A_{b\bar{b}}$ are shown in Table 4 and Figure 3. Because of limited statistics, we have not performed this measurement for $A_{c\bar{c}}$.

Mean $\sqrt{s}$	$A_{b\bar{b}}$
89.67 GeV	$0.025 \pm 0.051 \pm 0.007$
91.24 GeV	$0.097 \pm 0.017 \pm 0.007$
92.81 GeV	$0.062 \pm 0.042 \pm 0.007$

Table 4: $A_{b\bar{b}}$ for different center-of-mass energies. Note that the systematic error 0.007 is common to all energies.

Determination of $\sin^2\overline{\theta}_{\rm W}$

The Born level approximation given in the introduction is only valid at the Z^0 mass. In addition, one must apply QED initial and final state radiative corrections, as well as QCD corrections due to gluon bremsstrahlung. We use the ZFITTER program [18] to perform these corrections and extract $\sin^2\overline{\theta}_{\rm W}$. As input we use our measured values [19] of $m_{\rm Z} = 91.181 \pm 0.022$ GeV and $\Gamma_{\rm Z} = 2.501 \pm 0.017$ GeV, and the asymmetry values and energies given in Table 4. We obtain

$$\sin^2\overline{\theta}_{\rm W} = 0.2336 \pm 0.0029,$$

which is in excellent agreement with our measurement [19] of $\sin^2\overline{\theta}_{\rm W} = 0.2315 \pm 0.0025$ from

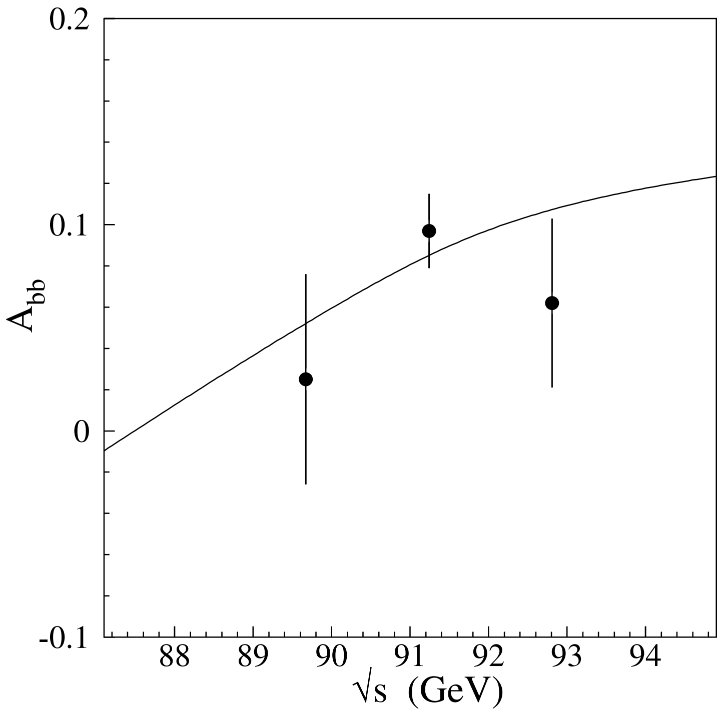

Figure 3: The energy dependence of $A_{\rm b\bar{b}}$ compared to the Standard Model expectation with $\sin^2\overline{\theta}_{\rm W} = 0.2336$.

the leptonic and hadronic decays of the Z^0. Figure 3 shows the measured energy dependence of $A_{\rm b\bar{b}}$ in comparison with the Standard Model expectation with $\sin^2\overline{\theta}_{\rm W} = 0.2336$. The Standard Model prediction for $A_{\rm c\bar{c}}$ is 0.056, in good agreement with our measurement.

As can be seen in Figure 3, the asymmetry predicted by the Standard Model is not linear as a function of energy, but rather flattens out above the Z^0 peak due to initial state radiation. We have used ZFITTER to take this effect into account, and to calculate the effective average center-of-mass energy for our complete data sample also taking into account the luminosity and cross-section at each energy. As most of our data was taken on the Z^0 peak, and as the effect is small, the effective average is the same as the peak energy: 91.24 GeV.

Conclusions

We have analyzed $Z^0 \to {\rm b\bar{b}}$ and $Z^0 \to {\rm c\bar{c}}$ decays using inclusive lepton events selected from a sample of 410,000 hadronic events. From a fit to the p and p_T distributions for single lepton and dilepton events, we have determined the $\mathrm{b\bar{b}}$ and $\mathrm{c\bar{c}}$ forward-backward asymmetries at the effective center-of-mass energy $\sqrt{s} = 91.24$ GeV to be

$$\begin{aligned} A_{\mathrm{b\bar{b}}} &= 0.086 \pm 0.015 \pm 0.007 \\ A_{\mathrm{c\bar{c}}} &= 0.083 \pm 0.038 \pm 0.027. \end{aligned}$$

Using the values of $A_{\mathrm{b\bar{b}}}$ obtained below, on, and above the Z^0 peak, we have determined $\sin^2\overline{\theta}_{\mathrm{W}}$ to be

$$\sin^2\overline{\theta}_{\mathrm{W}} = 0.2336 \pm 0.0029.$$

Acknowledgments

We wish to express our gratitude to the CERN accelerator divisions for the excellent performance of the LEP machine. We acknowledge the contributions of all the engineers and technicians who have participated in the construction and maintenance of this experiment. Those of us who are not from member states thank CERN for its hospitality and help.

The L3 Collaboration:

O.Adriani,[14] M.Aguilar-Benitez,[23] S.Ahlen,[9] H.Akbari,[5] J.Alcaraz,[15] A.Aloisio,[25] G.Alverson,[10] M.G.Alviggi,[25] G.Ambrosi,[30] Q.An,[16] H.Anderhub,[43] A.L.Anderson,[13] V.P.Andreev,[34] T.Angelov,[13] L.Antonov,[38] D.Antreasyan,[7] P.Arce,[23] A.Arefiev,[24] A.Atamanchuk,[34] T.Azemoon,[3] T.Aziz,[8,1] P.V.K.S.Baba,[16] P.Bagnaia,[33] J.A.Bakken,[32] L.Baksay,[39] R.C.Ball,[3] S.Banerjee,[8] J.Bao,[5] R.Barillère,[15] L.Barone,[33] R.Battiston,[30] A.Bay,[17] F.Becattini,[14] U.Becker,[13,43] F.Behner,[43] J.Behrens,[43] S.Beingessner,[4] Gy.L.Bencze,[11] J.Berdugo,[23] P.Berges,[13] B.Bertucci,[30] B.L.Betev,[38,43] M.Biasini,[30] A.Biland,[43] G.M.Bilei[30] R.Bizzarri,[33] J.J.Blaising,[4] B.Blumenfeld,[5] G.J.Bobbink,[15,2] M.Bocciolini,[14] R.Bock,[1] A.Böhm,[1] B.Borgia,[33] D.Bourilkov,[27] M.Bourquin,[17] D.Boutigny,[4] B.Bouwens,[2] E.Brambilla,[25] J.G.Branson,[35] I.C.Brock,[31] M.Brooks,[21] C.Buisson,[22] A.Bujak,[40] J.D.Burger,[13] W.J.Burger,[17] J.P.Burq,[22] J.Busenitz,[39] X.D.Cai,[16] M.Capell,[20] M.Caria,[30] G.Carlino,[25] F.Carminati,[14] A.M.Cartacci,[14] M.Cerrada,[23] F.Cesaroni,[33] Y.H.Chang,[13] U.K.Chaturvedi,[16] M.Chemarin,[22] A.Chen,[45] C.Chen,[6] G.M.Chen,[6] H.F.Chen,[18] H.S.Chen,[6] J.Chen,[13] M.Chen,[13] M.L.Chen,[3] W.Y.Chen,[16] G.Chiefari,[25] C.Y.Chien,[5] M.Chmeissani,[3] S.Chung,[13] C.Civinini,[14] I.Clare,[13] R.Clare,[13] T.E.Coan,[21] H.O.Cohn,[28] G.Coignet,[4] N.Colino,[15] A.Contin,[7] F.Crijns,[27] X.T.Cui,[16] X.Y.Cui,[16] T.S.Dai,[13] R.D'Alessandro,[14] R.de Asmundis,[25] A.Degré,[4] K.Deiters,[13] E.Dénes,[11] P.Denes,[32] F.DeNotaristefani,[33] M.Dhina,[43] D.DiBitonto,[39] M.Diemoz,[33] H.R.Dimitrov,[38] C.Dionisi,[33,15] M.T.Dova,[16] E.Drago,[25] T.Driever,[27] D.Duchesneau,[17] P.Duinker,[2] I.Duran,[36] H.El Mamouni,[22] A.Engler,[31] F.J.Eppling,[13] F.C.Erné,[2] P.Extermann,[17] R.Fabbretti,[41] M.Fabre,[41] S.Falciano,[33] S.J.Fan,[37] O.Fackler,[20] J.Fay,[22] M.Felcini,[15] T.Ferguson,[31] D.Fernandez,[23] G.Fernandez,[23] F.Ferroni,[33] H.Fesefeldt,[1] E.Fiandrini,[30] J.Field,[17] F.Filthaut,[27] G.Finocchiaro,[33] P.H.Fisher,[5] G.Forconi,[17] T.Foreman,[2] K.Freudenreich,[43] W.Friebel,[42] M.Fukushima,[13] M.Gailloud,[19] Yu.Galaktionov,[24,13] E.Gallo,[14] S.N.Ganguli,[8] P.Garcia-Abia,[23] S.S.Gau,[45] D.Gele,[22] S.Gentile,[33,15] S.Goldfarb,[10] Z.F.Gong,[18] E.Gonzalez,[23] P.Göttlicher,[1] A.Gougas,[5] D.Goujon,[17] G.Gratta,[29] C.Grinnell,[13] M.Gruenewald,[29] C.Gu,[16] M.Guanziroli,[16] J.K.Guo,[37] V.K.Gupta,[32] A.Gurtu,[15,8] H.R.Gustafson,[3] L.J.Gutay,[40] K.Hangarter,[1] A.Hasan,[16] D.Hauschildt,[2] C.F.He,[37] T.Hebbeker,[1] M.Hebert,[35] G.Herten,[13] U.Herten,[1] A.Hervé,[15] K.Hilgers,[1] H.Hofer,[43] H.Hoorani,[17] G.Hu,[16] G.Q.Hu,[37] B.Ille,[22] M.M.Ilyas,[16] V.Innocente,[15,25] H.Janssen,[15] S. Jezequel,[4] B.N.Jin,[6] L.W.Jones,[3] A.Kasser,[19] R.A.Khan,[16] Yu.Kamyshkov,[28] P.Kapinos,[34,42] J.S.Kapustinsky,[21] Y.Karyotakis,[15,4] M.Kaur,[16] S.Khokhar,[16] M.N.Kienzle-Focacci,[17] W.W.Kinnison,[21] D.Kirkby,[29] S.Kirsch,[42] W.Kittel,[27] A.Klimentov,[13,24] A.C.König,[27] E.Koffeman,[2] O.Kornadt,[1] V.Koutsenko,[13,24] A.Koulbardis,[34] R.W.Kraemer,[31] T.Kramer,[13] V.R.Krastev,[38,30] W.Krenz,[1] A.Krivshich,[34] H.Kuijten,[27] K.S.Kumar,[12] A.Kunin,[12,24] G.Landi,[14] D.Lanske,[1] S.Lanzano,[25] P.Lebrun,[22] P.Lecomte,[43] P.Lecoq,[15] P.Le Coultre,[43] D.M.Lee,[21] I.Leedom,[10] J.M.Le Goff,[15] R.Leiste,[42] M.Lenti,[14] E.Leonardi,[33] J.Lettry,[43] X.Leytens,[2] C.Li,[18,16] H.T.Li,[6] P.J.Li,[37] X.G.Li,[6] J.Y.Liao,[37] W.T.Lin,[45] Z.Y.Lin,[18] F.L.Linde,[15,2] B.Lindemann,[1] D.Linnhofer,[43] L.Lista,[25] Y.Liu,[16] W.Lohmann,[42,15] E.Longo,[33] Y.S.Lu,[6] J.M.Lubbers,[15] K.Lübelsmeyer,[1] C.Luci,[33] D.Luckey,[7,13] L.Ludovici,[33] L.Luminari,[33] W.Lustermann,[42] J.M.Ma,[6] W.G.Ma,[18] M.MacDermott,[43] P.K.Malhotra,[8†] R.Malik,[16] A.Malinin,[4,24] C.Maña,[23] D.N.Mao,[3] Y.F.Mao,[6] M.Maolinbay,[43] P.Marchesini,[43] F.Marion,[4] A.Marin,[9] J.P.Martin,[22] L.Martinez-Laso,[23] F.Marzano,[33] G.G.G.Massaro,[2] T.Matsuda,[13] K.Mazumdar,[8] P.McBride,[12] T.McMahon,[40] D.McNally,[43] Th.Meinholz,[1] M.Merk,[27] L.Merola,[25] M.Meschini,[14] W.J.Metzger,[27] Y.Mi,[16] G.B.Mills,[21] Y.Mir,[16] G.Mirabelli,[33] J.Mnich,[1] M.Möller,[1] B.Monteleoni,[14] R.Morand,[4] S.Morganti,[33] N.E.Moulai,[16] R.Mount,[29] S.Müller,[1] A.Nadtochy,[34] E.Nagy,[11] M.Napolitano,[25] H.Newman,[29] C.Neyer,[43] M.A.Niaz,[16] A.Nippe,[1] H.Nowak,[42] G.Organtini,[33] D.Pandoulas,[1] S.Paoletti,[14] P.Paolucci,[25] G.Passaleva,[14,30] S.Patricelli,[25] T.Paul,[5] M.Pauluzzi,[30] F.Pauss,[43] Y.J.Pei,[1] D.Perret-Gallix,[4] J.Perrier,[17] A.Pevsner,[5] D.Piccolo,[25] M.Pieri,[15,14] P.A.Piroué,[32] F.Plasil,[28] V.Plyaskin,[24] M.Pohl,[43] V.Pojidaev,[24,14] N.Produit,[17] J.M.Qian,[3] K.N.Qureshi,[16] R.Raghavan,[8] G.Rahal-Callot,[43] G.Raven,[2] P.Razis,[26] K.Read,[28] D.Ren,[43] Z.Ren,[16] M.Rescigno,[33] S.Reucroft,[10] A.Ricker,[1] S.Riemann,[42] O.Rind,[3] H.A.Rizvi,[16] F.J.Rodriguez,[23] B.P.Roe,[3] M.Röhner,[1] S.Röhner,[1] L.Romero,[23] J.Rose,[1] S.Rosier-Lees,[4] R.Rosmalen,[27] Ph.Rosselet,[19] A.Rubbia,[13] J.A.Rubio,[15] H.Rykaczewski,[43] M.Sachwitz,[42] E.Sajan,[30] J.Salicio,[15] J.M.Salicio,[23] G.S.Sanders,[21] A.Santocchia,[30] M.S.Sarakinos,[13] G.Sartorelli,[7,16] M.Sassowsky,[1] G.Sauvage,[4] V.Schegelsky,[34] K.Schmiemann,[1] D.Schmitz,[1] P.Schmitz,[1] M.Schneegans,[4] H.Schopper,[44] D.J.Schotanus,[27] S.Shotkin,[13] H.J.Schreiber,[42] J.Shukla,[31] R.Schulte,[1] S.Schulte,[1] K.Schultze,[1] J.Schütte,[12] J.Schwenke,[1] G.Schwering,[1] C.Sciacca,[25] I.Scott,[12] R.Sehgal,[16] P.G.Seiler,[41] J.C.Sens,[15,2] L.Servoli,[30] I.Sheer,[35] D.Z.Shen,[37] S.Shevchenko,[29] X.R.Shi,[29] E.Shumilov,[24] V.Shoutko,[24] E.Soderstrom,[32] A.Sopczak,[35] C.Spartiotis,[5] T.Spickermann,[1] P.Spillantini,[14] R.Starosta,[1] M.Steuer,[7,13] D.P.Stickland,[32] F.Sticozzi,[13] H.Stone,[17] K.Strauch,[12] B.C.Stringfellow,[40] K.Sudhakar,[8,1] G.Sultanov,[16] R.L.Sumner,[32] L.Z.Sun,[18,16] H.Suter,[43] R.B.Sutton,[31] J.D.Swain,[16] A.A.Syed,[16] X.W.Tang,[6] L.Taylor,[10] C.Timmermans,[27] Samuel C.C.Ting,[13] S.M.Ting,[13] M.Tonutti,[1] S.C.Tonwar,[8] J.Tóth,[11] A.Tsaregorodtsev,[34] G.Tsipolitis,[31] C.Tully,[29] K.L.Tung,[6] J.Ulbricht,[43] L.Urbán,[11] U.Uwer,[1] E.Valente,[33] R.T.Van de Walle,[27] I.Vetlitsky,[24] G.Viertel,[43] P.Vikas,[16] U.Vikas,[16] M.Vivargent,[4] H.Vogel,[31] H.Vogt,[42] I.Vorobiev,[24] A.A.Vorobyov,[34] L.Vuilleumier,[19] M.Wadhwa,[16] W.Wallraff,[1] C.R.Wang,[18] G.H.Wang,[31] J.H.Wang,[6] Q.F.Wang,[12] X.L.Wang,[18] Y.F.Wang,[14] Z.M.Wang,[16,18] A.Weber,[1] J.Weber,[43] R.Weill,[19] T.J.Wenaus,[20] J.Wenninger,[17] M.White,[13] C.Willmott,[23] F.Wittgenstein,[15] D.Wright,[32] R.J.Wu,[6] S.X.Wu,[16] Y.G.Wu,[6] B.Wysłouch,[13] Y.Y.Xie,[37] Y.D.Xu,[6] Z.Z.Xu,[18] Z.L.Xue,[37] D.S.Yan,[37] X.J.Yan,[13] B.Z.Yang,[18] C.G.Yang,[6] G.Yang,[16] K.S.Yang,[6] Q.Y.Yang,[6] Z.Q.Yang,[37] C.H.Ye,[16] J.B.Ye,[18] Q.Ye,[16] S.C.Yeh,[45] Z.W.Yin,[37] J.M.You,[16] N.Yunus,[16] M.Yzerman,[2] C.Zaccardelli,[29] P.Zemp,[43] M.Zeng,[16] Y.Zeng,[1] D.H.Zhang,[2] Z.P.Zhang,[18,16] B.Zhou,[9] J.F.Zhou,[1] R.Y.Zhu,[29] H.L.Zhuang,[6] A.Zichichi,[7,15,16] B.C.C.van der Zwaan.[2]

1 I. Physikalisches Institut, RWTH, W-5100 Aachen, FRG[§]
III. Physikalisches Institut, RWTH, W-5100 Aachen, FRG[§]
2 National Institute for High Energy Physics, NIKHEF, NL-1009 DB Amsterdam, The Netherlands
3 University of Michigan, Ann Arbor, MI 48109, USA
4 Laboratoire d'Annecy-le-Vieux de Physique des Particules, LAPP,IN2P3-CNRS, BP 110, F-74941 Annecy-le-Vieux CEDEX, France
5 Johns Hopkins University, Baltimore, MD 21218, USA
6 Institute of High Energy Physics, IHEP, Beijing, P.R. China
7 INFN-Sezione di Bologna, I-40126 Bologna, Italy
8 Tata Institute of Fundamental Research, Bombay 400 005, India
9 Boston University, Boston, MA 02215, USA
10 Northeastern University, Boston, MA 02115, USA
11 Central Research Institute for Physics of the Hungarian Academy of Sciences, H-1525 Budapest 114, Hungary
12 Harvard University, Cambridge, MA 02139, USA
13 Massachusetts Institute of Technology, Cambridge, MA 02139, USA
14 INFN Sezione di Firenze and University of Florence, I-50125 Florence, Italy
15 European Laboratory for Particle Physics, CERN, CH-1211 Geneva 23, Switzerland
16 World Laboratory, FBLJA Project, CH-1211 Geneva 23, Switzerland
17 University of Geneva, CH-1211 Geneva 4, Switzerland
18 Chinese University of Science and Technology, USTC, Hefei, Anhui 230 029, P.R. China
19 University of Lausanne, CH-1015 Lausanne, Switzerland
20 Lawrence Livermore National Laboratory, Livermore, CA 94550, USA
21 Los Alamos National Laboratory, Los Alamos, NM 87544, USA
22 Institut de Physique Nucléaire de Lyon, IN2P3-CNRS,Université Claude Bernard, F-69622 Villeurbanne Cedex, France
23 Centro de Investigaciones Energeticas, Medioambientales y Tecnologicas, CIEMAT, E-28040 Madrid, Spain
24 Institute of Theoretical and Experimental Physics, ITEP, Moscow, Russia
25 INFN-Sezione di Napoli and University of Naples, I-80125 Naples, Italy
26 Department of Natural Sciences, University of Cyprus, Nicosia, Cyprus
27 University of Nymegen and NIKHEF, NL-6525 ED Nymegen, The Netherlands
28 Oak Ridge National Laboratory, Oak Ridge, TN 37831, USA
29 California Institute of Technology, Pasadena, CA 91125, USA
30 INFN-Sezione di Perugia and Universitá Degli Studi di Perugia, I-06100 Perugia, Italy
31 Carnegie Mellon University, Pittsburgh, PA 15213, USA
32 Princeton University, Princeton, NJ 08544, USA
33 INFN-Sezione di Roma and University of Rome, "La Sapienza", I-00185 Rome, Italy
34 Nuclear Physics Institute, St. Petersburg, Russia
35 University of California, San Diego, CA 92182, USA
36 Dept. de Fisica de Particulas Elementales, Univ. de Santiago, E-15706 Santiago de Compostela, Spain
37 Shanghai Institute of Ceramics, SIC, Shanghai, P.R. China
38 Bulgarian Academy of Sciences, Institute of Mechatronics, BU-1113 Sofia, Bulgaria
39 University of Alabama, Tuscaloosa, AL 35486, USA
40 Purdue University, West Lafayette, IN 47907, USA
41 Paul Scherrer Institut, PSI, CH-5232 Villigen, Switzerland
42 DESY-Institut für Hochenergiephysik, O-1615 Zeuthen, FRG
43 Eidgenössische Technische Hochschule, ETH Zürich, CH-8093 Zürich, Switzerland
44 University of Hamburg, W-2000 Hamburg, FRG
45 High Energy Physics Group, Taiwan, ROC
§ Supported by the German Bundesministerium für Forschung und Technologie
† Deceased.

References

[1] S.L. Glashow, Nucl. Phys. . **22** (1961) 579;
S. Weinberg, Phys. Rev. Lett. **19** (1967) 1264;
A. Salam, "Elementary Particle Theory", Ed. N. Svartholm, Stockholm, "Almquist and Wiksell" (1968), 367.

[2] J. Kühn and P. Zerwas, "Heavy Flavors at LEP I" Preprint MPI-PAE/PTh 49/89, Max Planck Institute, Munich. A shortened version is available as J. Kühn and P. Zerwas in "Z Physics at LEP I", CERN 89-08, ed. G. Altarelli *et al.*, (CERN, Geneva, 1989), volume 1, pp. 267–372.

[3] M. Böhm and W. Hollik, in "Z Physics at LEP I", CERN 89-08, ed. G. Altarelli *et al.*, (CERN, Geneva, 1989), volume 1, pp. 203–234.

[4] MARK II Collab., J.F. Kral *et al.*, Phys. Rev. Lett. **64** (1990) 1211.

[5] L3 Collab., B. Adeva *et al.*, Phys. Lett. **B 252** (1991) 713.

[6] OPAL Collab, M.Z. Akrawy *et al.*, Phys. Lett. **B 263** (1991) 311.

[7] ALEPH Collab., D. Decamp *et al.*, Phys. Lett. **B 263** (1991) 325.

[8] DELPHI Collab., P. Abreu *et al.*, Phys. Lett. **B 276** (1992) 536.

[9] L3 Collab., B. Adeva *et al.*, An Improved Measurement of B^0-$\bar{B}^0$ Mixing in Z^0 Decays, Preprint CERN-PPE/92-84, CERN, 1992, submitted to Physics Letters B.

[10] L3 Collab., B. Adeva *et al.*, Nucl. Inst. Meth. **A 289** (1990) 35.

[11] L3 Collab., B. Adeva *et al.*, Phys. Lett. **B 252** (1990) 703.

[12] T. Sjöstrand and M. Bengtsson, Comput. Phys. Commun. **43** (1987) 367,
T. Sjöstrand in "Z Physics at LEP1", CERN-89-08, ed. G. Altarelli *et al.*, (CERN, Geneva, 1989), volume 3, pp. 143–340.
For 1990 data we used JETSET 7.2 and for 1991 data we used JETSET 7.3.

[13] C. Peterson *et al.*, Phys. Rev. **D 27** (1983) 105.

[14] The L3 detector simulation is based on GEANT Version 3.14.
See R. Brun *et al.*, "GEANT 3", CERN DD/EE/84-1 (Revised), September 1987.
The GHEISHA program (H. Fesefeldt, RWTH Aachen Report PITHA 85/02 (1985)) is used to simulate hadronic interactions.

[15] L3 Collab., B. Adeva *et al.*, Phys. Lett. **B 261** (1991) 177.

[16] Particle Data Group, Phys. Lett. **B 239** (1990) VII.113, We have averaged the PETRA and PEP measurements according to the procedure used by the Particle Data Group.

[17] O. Adriani *et al.*, Nucl. Inst. Meth. **A 302** (1991) 53.

[18] D. Bardin *et al.*, Z. Phys. **C 44** (1989) 493, Nucl. Phys. **B 351** (1991) 1 and Phys. Lett. **B 255** (1991) 290.

[19] L3 Collab., B. Adeva *et al.*, Z. Phys. **C 51** (1991) 179.